International Journal of Antimicrobial Agents 65 (2025) 107441

Contents lists available at ScienceDirect

International Journal of Antimicrobial Agents

journal homepage: www.elsevier.com/locate/ijantimicag

Short Communication

Plasma effects on bacterial time-kill dynamics: Insights from a PK/PD modelling analysis

Salma M Bahnasawy[a], Hifza Ahmed[b], Markus Zeitlinger[b], Lena E Friberg[a], Elisabet I Nielsen[a,*]

[a] Department of Pharmacy, Uppsala University, Uppsala, Sweden
[b] Department of Clinical Pharmacology, Medical University of Vienna, Vienna, Austria

ARTICLE INFO

Article history:
Received 27 August 2024
Accepted 30 December 2024

Editor: Dr Y-W Lin

Key words:
Time-kill curve (TKC)
Pharmacokinetics-pharmacodynamics (PKPD)
Plasma protein binding (PPB)

ABSTRACT

In vitro time-kill curve (TKC) experiments are an important part of the pharmacokinetic- pharmacodynamic (PKPD) characterisation of antibiotics. Traditional TKCs use Mueller-Hinton broth (MHB), which lacks specific plasma components that could potentially influence the bacterial growth and killing dynamics, and affect translation to *in vivo*. This study aimed to evaluate the impact of plasma on the PKPD characterisation of two antibiotics; cefazolin and clindamycin. TKC experiments were conducted in pure MHB, and MHB spiked with 20% and 70% human plasma. Plasma protein binding (PPB) data were available, and a linear model described cefazolin's PPB, while clindamycin's PPB was best described by a second-order polynomial model. PKPD models were developed based on pure MHB and described drug effects using an E_{max} model, with consideration of adaptive resistance for cefazolin. The observed bacterial growth and killing in the plasma-spiked MHB TKC data was insufficiently described when applying the developed PPB and PKPD models. In plasma spiked MHB, a growth delay was observed, estimated to 0.25 h (20% plasma), or 2.90 h (70% plasma) for cefazolin, and 0.64 h (20% plasma), or 1.40 h (70% plasma) for clindamycin. Furthermore, the drug effect was higher than expected in plasma-spiked MHB, with bacterial stasis and/or killing at unbound concentrations below MIC, necessitating drug effect parameter scaling (C_{50} for cefazolin, Hill coefficient for clindamycin). The findings highlight significant differences in bacterial growth and killing dynamics between pure MHB and plasma-spiked MHB and exemplify how PKPD modelling may be used to improve the translation of *in vitro* results.

1. Introduction

In vitro time-kill curve (TKC) experiments are essential for studying the pharmacokinetic- pharmacodynamic (PKPD) relationship of antibiotics. They provide insights into antibiotic activity that can potentially be translated to *in vivo* effects through PKPD modelling [1].

Traditionally, pure Mueller–Hinton broth (MHB) is used as the standard medium in these experiments providing an ideal bacterial growth environment with good reproducibility [2]. Nevertheless, MHB lacks resemblance to the *in vivo* environment, where the presence of protein binding and other biological factors may influence bacterial growth and the antibiotic-bacteria interaction [3].

Several studies have investigated the potential impact of the growth media on antibiotic-induced bacterial killing (e.g. MHB spiked with plasma, or other body fluids, such as urine, cerebrospinal fluid, or bile) [2]. Commonly, the results are analysed as changes in MIC [4], and/or differences in the bacterial count at a certain time point post-inoculation [5,6]. However, there is limited knowledge on how the growth media influence the time course of bacterial growth and antibiotic effect.

Human plasma has a complex composition. It is well known that plasma protein binding (PPB) reduces the unbound and pharmacologically active drug concentration. When translating *in vitro* results, the expected fraction unbound (f_u) is typically used to predict *in vivo* unbound drug concentrations. Other aspects of the PKPD relationship are typically assumed to be the same as observed *in vitro* [7].

Cefazolin and clindamycin are among the examples of highly protein-bound antibiotics with non-linear saturable binding at higher concentrations [8,9]. Cefazolin binds primarily to albumin,

* Corresponding author. Mailing address: Department of Pharmacy, Uppsala University, Box 580, 75123 Uppsala, Sweden.
E-mail address: elisabet.nielsen@farmaci.uu.se (E.I. Nielsen).

https://doi.org/10.1016/j.ijantimicag.2024.107441

while clindamycin binds predominantly to alpha-1-acid glycoprotein, with binding percentages ranging 52–85 % for cefazolin, and 62-81% for clindamycin [8,9].

This analysis aimed to evaluate the bacterial growth and PKPD of cefazolin and clindamycin in time-kill experiments conducted *in vitro* across MHB spiked with varying concentrations of human plasma. By integrating data on PPB, this research sought to elucidate the impact of human plasma on the antibacterial efficacy assessment. Thereby exploring how the growth environment could impact the translational capacity of PKPD models for antibiotics.

2. Methods

2.1. Data

2.1.1. Plasma protein binding

This analysis incorporated equilibrium dialysis data on PPB for cefazolin and clindamycin measured at clinically achievable antibiotic concentrations (2.5, 25 µg/mL for cefazolin, and 2, 5, 20 µg/mL for clindamycin). The experiments were performed in 0.01 M phosphate-buffered saline (PBS) spiked with 20% and 70% of pooled human plasma. Details of the experimental procedure have been described earlier [10,11].

2.1.2. In vitro *time-kill curve experiments*

Escherichia coli (ATCC 25922) with MIC of 2 µg/mL was used for cefazolin, and *Staphylococcus aureus* (ATCC 29213) with MIC of 0.125 µg/mL was used for clindamycin. Antibiotic concentrations ranged between 0.25–16 µg/mL for cefazolin and 0.0156-16 µg/mL for clindamycin. For each drug, the experiments were run in three different growth media; pure MHB, MHB spiked with 20% human plasma, and MHB spiked with 70% human plasma. Samples for bacterial counts were taken at 0, 1, 2, 3, 4, 8, 24 h post-inoculation, and colony forming units (CFUs) were determined by plating serial dilutions onto Columbia agar plates followed by manual counting. Each experiment was repeated three times with duplicate sampling at each sampling time point. The lower limit of quantification (LOQ) was 200 CFU/mL.

2.2. Modelling workflow

The modelling workflow involved four main steps; 1) developing PPB models, 2) developing PKPD models based on TKC experiments in pure MHB, 3) Application of combined PPB and PKPD models to plasma-spiked TKC experiments, 4) Exploration of PKPD differences between MHB and plasma-spiked TKC experiments

2.2.1. Developing PPB models

A regression analysis was performed for each antibiotic based on the observed total and unbound concentration data. Different models were tested including linear, polynomial, and exponential models with model selection based on the sum of residuals and visual fit. The PPB models described fu as a function of the total drug concentration assessed at 20% and 70% plasma.

2.2.2. Developing PKPD models based on TKC experiments in pure MHB

For PKPD model development, initially, only data from the TKC experiments run in pure MHB were considered. The bacteria were assumed to be present in a growing drug-susceptible (S), or resting drug-insusceptible stage (R) as described previously [12]. Growth-related parameters (k_g, k_d, and B_{max}) were first estimated based on the data from the growth control data. Additionally, a bacterial growth delay was tested according to Sou et al. [7] with estimation of the bacterial delay (T_{50}) according to:

$$k_{g(time)} = k_{g(\text{maximum})} \times \frac{Time^5}{T_{50}^5 + Time^5}$$

The drug effect was described by an additive sigmoidal E_{max} model allowing an increase in the bacterial killing rate [12]. In case of signs of bacterial regrowth, adaptive resistance models were tested by allowing a drug-dependent decrease in the maximal killing rate (E_{max}) or in drug potency (i.e. higher C_{50}) [13].

Observations below the LOQ (BLOQ) were treated as censored data, by implementing the M3 method [14]. Additionally, potential correlations among residual errors for replicate samples were handled using the NONMEM L2 data item [15]. Both the observed data and model predictions were $\log_{10}$ transformed and additive residual error models on the log-scale were used. Model selection was based on the objective functions value (OFV) using the likelihood ratio test for nested models at a predefined P-value $<$0.001. Model performance was evaluated based on visual predictive checks (VPCs).

2.2.3. Applying the models to plasma-spiked TKC experiments

The developed PPB and PKPD models were combined and applied (without re-estimation, i.e. MAXEVAL=0) to plasma-spiked TKCs. The model performance was evaluated by VPCs.

2.2.4. Exploration of PKPD differences between MHB and plasma-spiked TKC experiments

If the combined PPB and PKPD model failed to adequately predict the observed bacterial dynamics in plasma-spiked media, the PKPD model was re-evaluated. First, the bacterial growth was allowed to be re-estimated, including exploring a potential growth delay. Thereafter, the drug effect parameters (i.e. E_{max}, C_{50}, γ) were sequentially tested for scaling as follows;

$$Parameter_{x\%\ plasma} = Parameter_{MHB} \times SF$$

where the $Parameter_{x\%\ plasma}$ is the parameter value in media spiked with x% plasma, $Parameter_{MHB}$ is the parameter value estimated in pure MHB, SF is a fractional scaling factor. This procedure has been described earlier by Aranzana-Climent et al., implemented using a forward inclusion, backward elimination procedure [16]. This involves a forward addition step where the SF parameters were unfixed (default value is 1) one by one until no significant improvement in OFV (drop by 3.84 points, $P < 0.05$). Then, a backward elimination was performed, where the SF parameters were fixed to 1 one by one until significant worsening in OFV (increase by 10.83 points, $P < 0.001$). In both steps, the PKPD parameters were fixed to MHB estimates, and residual errors were allowed to be estimated.

2.3. Software

Data management, graphical presentations, and regression analyses were performed in R version 4.2.0 with the help of tidyverse, xpose4, and aomisc packages. Model estimation was performed using a nonlinear mixed-effects modelling in NONMEM version 7.5 (ICON Development Solutions, Ellicott City, MD, United States). Model runs were executed using Perl-Speaks-NONMEM 5.3.0 (PsN), Pirana 2.9.9.

3. Results

3.1. Plasma protein binding models

The concentration-dependent PPB of cefazolin was described by linear functions for both the 20% and 70% plasma-spiked media with an expected fu range of 40–44% (20% plasma), and 15–17% (70% plasma) in the TKCs. Clindamycin PPB data were best described by second-order polynomial models resulting in TKCs fu range of 14–39% (20% plasma), and 2.2–18% (70% plasma). Further

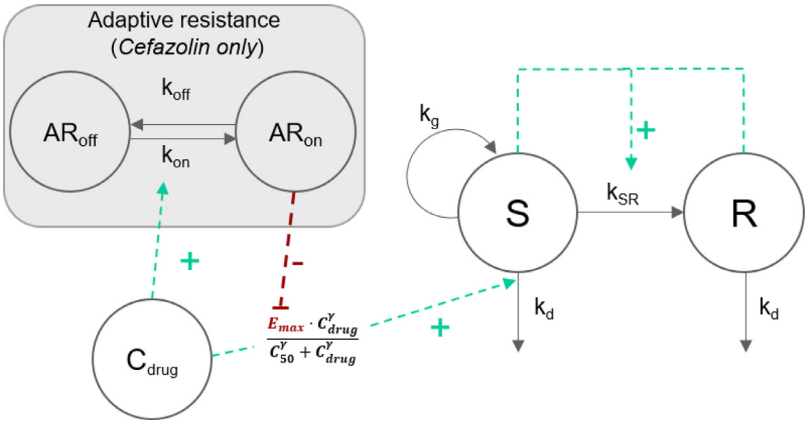

Figure 1. PKPD model schematic for cefazolin and clindamycin. S: bacteria in a growing drug-susceptible phase, R: bacteria in resting insusceptible phase. Adaptive resistance (AR) compartments (grey shaded) were implemented only for cefazolin. Dashed lines indicate stimulatory functions (green), or inhibitory functions (red). Parameter descriptions are supplied in Table 1.

Table 1
Final model parameter estimates with relative standard error in percent

Parameter (unit)	Description	Pure MHB	20% plasma-spiked MHB	70% plasma-spiked MHB
Cefazolin				
k_g (h^{-1})	Rate constant of bacterial growth	1.92 (9%)	1.92 (fixed)	
k_d (h^{-1})	Rate constant of natural bacterial death	0.179 (fixed)	0.179 (fixed)	
T_{50} (h)	Time to reach 50% of k_g maximum value	-	0.252 (58%)	2.87 (11%)
B_{max} (log_{10} CFU/mL)	Maximal bacterial load	10.0 (1%)	10.0 (fixed)	
Inoculum (log_{10} CFU/mL)	Initial bacterial load	6.61 (2%)	6.56 (1%)	6.59 (2%)
E_{max} (h^{-1})	Maximum rate constant for drug effect	7.35 (11%)	7.35 (fixed)	
C_{50} (mg/L)	Drug concentration needed to achieve 50% of E_{max}	3.98 (18%)	3.98 (fixed)	
γ (-)	Sigmoidicity factor for E_{max} function	1.0 (fixed)	1.0 (fixed)	
SF_{C50} (-)	Fractional scaling factor for C_{50}	-	0.796 (2%)	0.349 (5%)
k_{on} ($L \cdot h^{-1} \cdot mg^{-1}$)	Rate constant for onset of adaptive resistance	0.0249 (35%)	0.0249 (fixed)	
k_{off} (h^{-1})	Rate constant for reversal of adaptive resistance	0.0139 (fixed)	0.0139 (fixed)	
AR_{50} (-)	The fraction in adaptive resistance compartment needed to reduce E_{max} by 50%	0.635 (23%)	0.635 (fixed)	
$\sigma^2_{bacterial\ count}$ (log_{10} CFU/mL)	Additive residual error variance of bacterial count (on log_{10} scale)	0.403 (14%)	0.245 (14%)	0.926 (15%)
$\sigma^2_{replicate}$ (log_{10} CFU/mL)	Additive residual error variance of replicate (on log_{10} scale)	0.00549 (14%)	0.00719 (14%)	0.0124 (14%)
Clindamycin				
k_g (h^{-1})	Rate constant of bacterial growth	1.38 (17%)	0.958 (2%)	0.895 (2%)
k_d (h^{-1})	Rate constant of natural bacterial death	0.179 (fixed)	0.179 (fixed)	
T_{50} (h)	Time to reach 50% of k_g maximum value	-	0.636 (43%)	1.40 (22%)
B_{max} (log_{10} CFU/mL)	Maximal bacterial load	9.56 (1%)	9.59 (2%)	9.08 (2%)
Inoc (log_{10} CFU/mL)	Initial bacterial load	6.96 (1%)	6.55 (1%)	6.51 (1%)
E_{max} (h^{-1})	Maximum rate constant for drug effect	1.50 (15%)	1.50 (fixed)	
C_{50} (mg/L)	Drug concentration needed to achieve 50% of E_{max}	0.0236 (26%)	0.0236 (fixed)	
γ (-)	Sigmoidicity factor for E_{max} function	1.0 (fixed)	1.0 (fixed)	
SF_{γ} (-)	Fractional scaling factor for γ	-	0.243 (5%)	0.221 (6%)
$\sigma^2_{bacterial\ count}$ (log_{10} CFU/mL)	Additive residual error variance of bacterial count (on log_{10} scale)	0.239 (26%)	0.233 (12%)	0.296 (14%)
$\sigma^2_{replicate}$ (log_{10} CFU/mL)	Additive residual error variance of replicate (on log_{10} scale)	0.00208 (10%)	0.00477 (18%)	0.00297 (14%)

details on the final PPB models and model-predicted unbound concentrations in all TKCs at different media are provided in the supplementary data Table 1S, and Fig. 1S.

3.2. PKPD models

A schematic of the developed PKPD models, based on MHB TKC data, is depicted in Fig. 1, and the final model parameter estimates are provided in Table 1. The drug effect was best described by basic E_{max} models (γ=1) for both drugs. Bacterial regrowth was observed at 24 h for cefazolin concentrations equal to MIC. The model captured this as adaptive resistance allowing E_{max} to decrease with drug exposure. A lag in bacterial growth was observed with the plasma-spiked MHB, but not pure MHB (cefazolin; 0.25 h (20% plasma), 2.90 h (70% plasma), clindamycin; 0.64 h (20% plasma), 1.40 h (70% plasma)). Applying the developed PKPD and PPB models to plasma-spiked MHB data was deemed to be insufficient to describe the observed bacterial growth and killing (Fig. 2S), indicating the need for parameter scaling. C_{50} of cefazolin was scaled with an estimated SF of 0.80 (20% plasma) and 0.35 (70% plasma). Clindamycin PD was best described by scaling the sigmoidicity factor (γ) with an estimated SF of 0.24 (20% plasma) and 0.22 (70% plasma). VPCs of the final models are shown in Fig. 2. The model codes and plots of the raw data

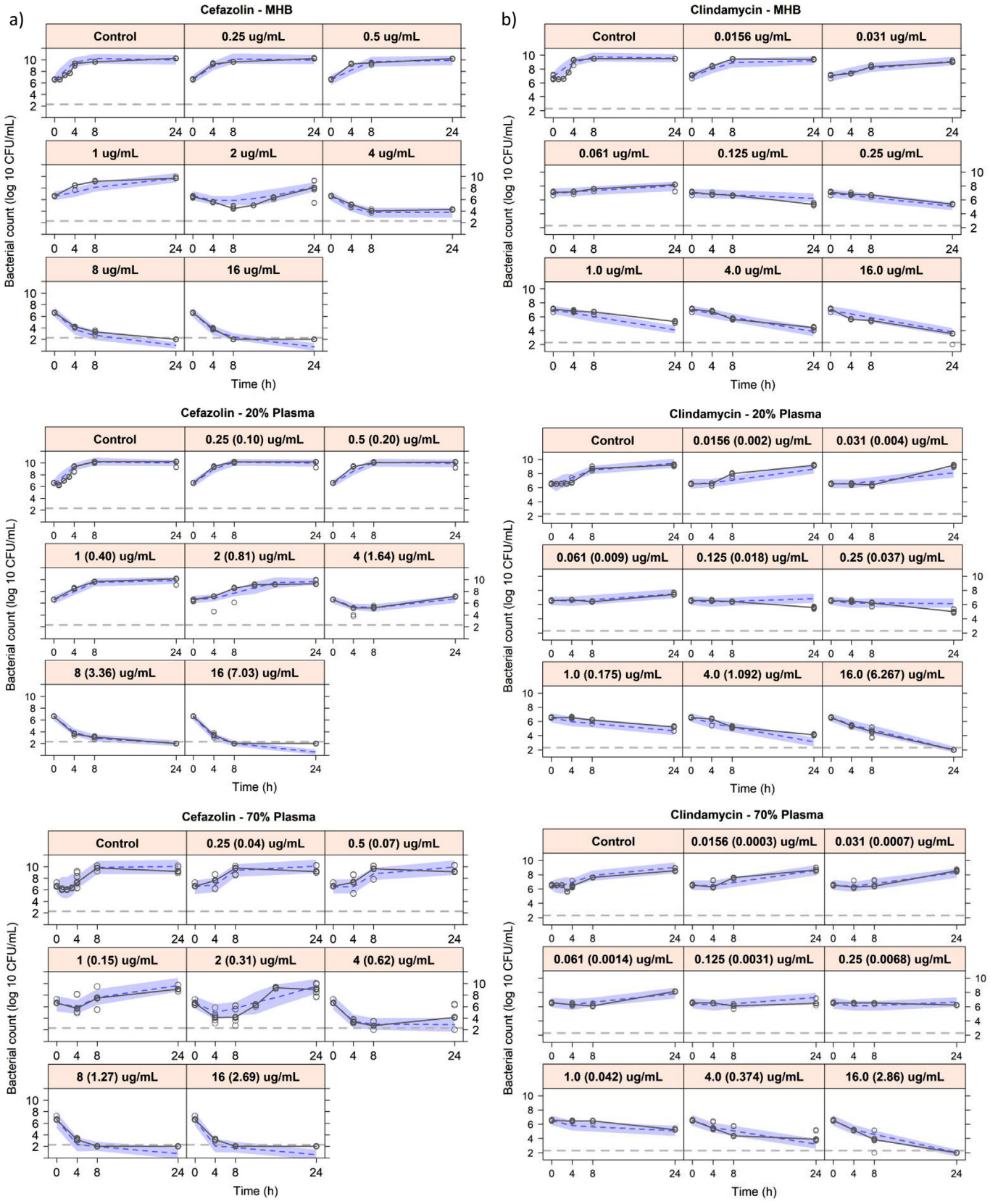

Figure 2. Visual predictive checks of the final models of *in vitro* time-kill curves for cefazolin (a), and clindamycin (b) when performed in pure Mueller–Hinton broth (top), and with 20% plasma (middle), and 70% plasma (bottom). Each subplot depicts the time course of bacterial dynamics at different total antibiotic concentrations, where the unbound concentration is provided in brackets for the plasma-spiked media. The grey open circles represent the observed data. The grey solid lines represent the median of the observations, and the blue dashed lines represent the median of simulated bacterial counts. The blue shaded areas correspond to the 95% confidence interval for the simulated median. The dashed grey lines represent the lower limit of quantification.

from the TKC experiments (Figures 3S and 4S) are provided in the supplementary material.

4. Discussion

This analysis aimed to evaluate the impact of human plasma on bacterial growth and killing dynamics as observed in *in vitro* TKC experiments using a modelling approach. Our results highlight bacterial growth delays in the presence of plasma, which were more pronounced at higher plasma concentrations. Additionally, in the presence of plasma, the antibacterial effect was higher than expected, with bacterial stasis and/or killing observed also at low unbound antibiotic concentrations (i.e. below the MIC) (Fig. 2S).

In the current analysis, we applied the developed MHB-based PKPD models to plasma-spiked TKC data, assuming only the unbound drug concentration to have killing activity. However, this approach was insufficient to capture the bacterial killing at unbound concentrations below the MIC (Fig. 2S). The need for scaling the drug effect parameters suggests that factors beyond unbound drug concentration may play a role in bacterial killing. The scaling of C_{50} (for cefazolin) might not reflect a direct change in drug susceptibility but rather unobserved underlying mechanisms that potentiate the bacterial killing in the presence of plasma. For instance, nutrient deprivation, bacterial phenotypic changes, or complement system activation could potentially develop in plasma whereas they may be mostly absent in pure MHB.

Phenotypical differences between bacteria grown in nutrient-rich media and *in vivo* can affect growth rates and antibiotic efficacy, with lower growth rates *in vivo* [17]. Notably, the complement system's activation in plasma-spiked media can enhance bacterial killing via membrane attack complex formation [18]. Previous studies have highlighted this potential activation *in vitro* (plasma/serum) [19,20]. This could be one possible mechanism for the enhanced bacterial killing at low unbound antibiotic concentrations observed in our study.

It is important to acknowledge that *in vivo* environments typically have complex dynamic conditions that are not replicated in the current experimental setup. For instance, *in vivo*, bacteria can reside in diverse environments beyond plasma, such as interstitial fluids and tissues, which differ in nutrient availability, pH, and immune factors, affecting bacterial growth and antibiotic efficacy. Factors like blood flow, tissue penetration, and the dynamic interplay between bacteria, antibiotics, and the host can further impact bacterial dynamics.

In this analysis, we focused on clinically relevant concentrations for assessing the protein binding of the two drugs. This range did not cover the full concentration range in the TKC experiments, especially in the lower range, which is a limitation of this study. While the included data provide valuable insights into PKPD relationships in the context of protein binding, future studies are needed to explore the non-linear protein binding in more detail. Furthermore, this study used PBS for PPB experiments to avoid interference in the HPLC analysis. Future experiments are warranted to assess the comparability of PPB in PBS and MHB.

In conclusion, the present findings highlight significant differences in bacterial growth and killing dynamics between pure MHB and plasma-spiked MHB. Further research is warranted to explore the underlying mechanisms by which plasma components affect bacterial dynamics and antibiotic efficacy. By integrating more complex biological factors into PKPD modelling, we can improve the prediction and optimisation of antibiotic therapy in clinical practice. This study provides a foundation for further exploration into the effects of *in vivo* environment on antibiotic action, paving the way for more accurate and reliable *in vitro - in vivo* translation of antibiotic activity.

Declaration of competing interest

The authors declare that they have no known competing financial interests or personal relationships that could have appeared to influence the work reported in this paper.

Funding

This project was funded by the EU's Horizon 2020 program under the Marie Skłodowska-Curie grant No 861323. Salma Bahnasawy and Hifza Ahmed were members of the TIPAT consortium during this work.

Ethical approval

Not required.

Randomized controlled Trial

Not applicable.

The study involves sequences

Not applicable.

Declaration of generative AI in scientific writing

During the preparation of this manuscript, Salma Bahnasawy used Chatgpt to help with scientific writing and increase the content readability. After using this tool, all authors reviewed and edited the content as needed and take full responsibility for the content of the publication.

Supplementary materials

Supplementary material associated with this article can be found, in the online version, at doi:10.1016/j.ijantimicag.2024.107441.

References

[1] Nielsen EI, Friberg LE. Pharmacokinetic-pharmacodynamic modeling of antibacterial drugs. Pharmacol Rev 2013;65:1053–90. doi:10.1124/pr.111.005769.
[2] Nussbaumer-Pröll A, Zeitlinger M. Use of supplemented or human material to simulate PD behavior of antibiotics at the target site in vitro. Pharmaceutics 2020;12:773. doi:10.3390/pharmaceutics12080773.
[3] Satta G, Cornaglia G, Foddis G, Pompei R. Evaluation of ceftriaxone and other antibiotics against Escherichia coli, Pseudomonas aeruginosa, and Streptococcus pneumoniae under in vitro conditions simulating those of serious infections. Antimicrob Agents Chemother 1988;32:552–60.
[4] Zeitlinger MA, Sauermann R, Traunmüller F, Georgopoulos A, Müller M, Joukhadar C. Impact of plasma protein binding on antimicrobial activity using time–killing curves. J Antimicrob Chemother 2004;54:876–80. doi:10.1093/jac/dkh443.
[5] Zeitlinger M, Sauermann R, Fille M, Hausdorfer J, Leitner I, Muller M. Plasma protein binding of fluoroquinolones affects antimicrobial activity. Journal of Antimicrob Chemother 2008;61:561–7. doi:10.1093/jac/dkm524.
[6] Burian A, Wagner C, Stanek J, Manafi M, Bohmdorfer M, Jager W, et al. Plasma protein binding may reduce antimicrobial activity by preventing intra-bacterial uptake of antibiotics, for example clindamycin. J Antimicrob Chemother 2011;66:134–7. doi:10.1093/jac/dkq400.
[7] Sou T, Hansen J, Liepinsh E, Backlund M, Ercan O, Grinberga S, et al. Model-informed drug development for antimicrobials: translational PK and PK/PD modeling to predict an efficacious human dose for apramycin. Clin Pharmacol Ther 2021;109:1063–73. doi:10.1002/cpt.2104.
[8] Vella-Brincat JWA, Begg EJ, Kirkpatrick CMJ, Zhang M, Chambers ST, Gallagher K. Protein binding of cefazolin is saturable in vivo both between and within patients. Br J Clin Pharmacol 2007;63:753–7. doi:10.1111/j.1365-2125.2006.02827.x.

[9] Kays MB, White RL, Gatti G, Gambertoglio JG. Ex vivo protein binding of clindamycin in sera with normal and elevated alpha 1-acid glycoprotein concentrations. Pharmacotherapy 1992;12:50–5.
[10] Ahmed H, Böhmdorfer M, Eberl S, Jäger W, Zeitlinger M. Interspecies variability in protein binding of antibiotics basis for translational PK/PD studies—A case study using cefazolin. Antimicrob Agents Chemother 2024;68:e01647 e01623. doi:10.1128/aac.01647-23.
[11] Ahmed H, Böhmdorfer M, Jäger W, Zeitlinger M. Insights into interspecies protein binding variability using clindamycin as an example. J Antimicrob Chemother 2024. doi:10.1093/jac/dkae412.
[12] Nielsen EI, Viberg A, Löwdin E, Cars O, Karlsson MO, Sandström M. Semimechanistic pharmacokinetic/pharmacodynamic model for assessment of activity of antibacterial agents from time-kill curve experiments. Antimicrob Agents Chemother 2007;51:128–36. doi:10.1128/AAC.00604-06.
[13] Mohamed AF, Nielsen EI, Cars O, Friberg LE. Pharmacokinetic-pharmacodynamic model for gentamicin and its adaptive resistance with predictions of dosing schedules in new born infants. Antimicrob Agents Chemother 2012;56:179–88. doi:10.1128/aac.00694-11.
[14] Beal SL. Ways to fit a PK model with some data below the quantification limit. J Pharmacokinet Pharmacodyn 2001;28:481–504. doi:10.1023/A:1012299115260.
[15] Karlsson MO, Beal SL, Sheiner LB. Three new residual error models for population PK/PD analyses. J Pharmacokinet Biopharm 1995;23:651–72. doi:10.1007/BF02353466.
[16] Aranzana-Climent V, Hughes D, Cao S, Tomczak M, Urbas M, Zabicka D, et al. Translational in vitro and in vivo PKPD modelling for apramycin against Gram-negative lung pathogens to facilitate prediction of human efficacious dose in pneumonia. Clin Microbiol Infect 2022;28:1367–74. doi:10.1016/j.cmi.2022.05.003.
[17] Brown MRW, Williams P. The influence of environment on envelope properties affecting survival of bacteria in infections. Annu Rev Microbiol 1985;39:527–56. doi:10.1146/annurev.mi.39.100185.002523.
[18] Walport Mark J. Complement. N Eng J Med 2001;344:1058–66. doi:10.1056/NEJM200104053441406.
[19] Kirschfink M, Mollnes TE. Modern complement analysis. Clin Diagn Lab Immunol 2003;10:982–9. doi:10.1128/CDLI.10.6.982-989.2003.
[20] Pfeifer PH, Kawahara MS, Hugli TE. Possible mechanism for in vitro complement activation in blood and plasma samples: FUTHAN/EDTA controls in vitro complement activation. Clin Chem 1999;45:1190–9. doi:10.1093/clinchem/45.8.1190.